Eq 21, we use the cylindrical coordinate where $d\bar{r}_{12} = r_{12}dr_{12}dz_{12}d\theta$. We also use the definition of $\rho^{(2)}$ with respect to the radial- (or pair-) distribution function as g. Since the radial distribution function of hard-spheres is only a function of the distance $(r_{12}^2 + z_{12}^2)^{0.5}$ between the two molecules, then we can write

$$\rho^{(2)} = \rho(z_1)\rho(z_2)g_{hs}\left((r_{12}^2 + z_{12}^2)^{\frac{1}{2}}\right). \tag{28}$$

Then Eq. 21 will be in the following form,

$$P_{zz}^{FF} = -\frac{1}{2}\iiint \varphi'_{hs}\left((r_{12}^2 + z_{12}^2)^{\frac{1}{2}}\right)\rho_{hs}(z_1)\rho_{hs}(z_2)g_{hs} \times \left((r_{12}^2 + z_{12}^2)^{\frac{1}{2}}\right)\frac{z_{12}^2}{(r_{12}^2 + z_{12}^2)^{\frac{1}{2}}}r_{12}dr_{12}dz_{12}d\theta, \tag{29}$$

where $\rho_{hs}(z_i)$ is the local density of hard-spheres, $g_{hs}\left((r_{12}^2 + z_{12}^2)^{\frac{1}{2}}\right)$ is the hard-sphere radial-distribution function, which is angle-independent but it depends on the distance between molecules, $(r_{12}^2 + z_{12}^2)^{\frac{1}{2}}$. As a result Eq. 29 reduces to

$$P_{zz}^{FF} = -\pi\iint \varphi'_{hs}\left((r_{12}^2 + z_{12}^2)^{\frac{1}{2}}\right)(\rho_{hs}(z_1)\rho_{hs}(z_2)g_{hs} \times \left((r_{12}^2 + z_{12}^2)^{\frac{1}{2}}\right)\frac{z_{12}^2}{(r_{12}^2 + z_{12}^2)^{\frac{1}{2}}}r_{12}dr_{12}dz_{12} \tag{30}$$

We select the position of molecule 1 (fixed) on the center of coordinate, therefore the coordinates of the distance between two molecules z_{12} and r_{12} are replaced with $z_{12} = z_2$, $dz_{12} = dz_2$, $r_{12} = r_2$, and $dr_{12} = dr_2$. Then we can write Eq. 30 as:

$$P_{zz}^{FF} = -\pi\rho_{hs}(z_1)\iint \varphi'_{hs}((r_2^2 + z_2^2)^{0.5})\rho_{hs}(z_1)\rho_{hs}(z_2)g_{hs} \times ((r_2^2 + z_2^2)^{0.5})\frac{z_2^2}{(r_2^2 + z_2^2)^{0.5}}r_2dr_2dz_2 \tag{31}$$

For the hard-sphere potential $\varphi'_{hs}((r_2^2 + z_2^2)^{0.5})$ is zero everywhere except at $(r_2^2 + z_2^2)^{0.5} = \sigma$. Therefore, to solve Eq. 31 we use the following definition.

$$\varphi'(r) = \delta\left((r_2^2 + z_2^2)^{0.5} - \sigma\right)(-kT)\exp\left(\frac{\varphi_{hs}((r_2^2 + z_2^2)^{0.5})}{kT}\right), \tag{32}$$

where $\delta((r_2^2 + z_2^2)^{0.5}-\sigma)$ is the Dirac delta-function. By inserting Eq. 32 into Eq. 31 we get:

$$P_{zz}^{FF} = \pi kT\rho_{hs}(z_1)\left[\int_{-\sigma}^{+\sigma}\rho_{hs}(z_2)\frac{z_2^2}{(r_2^2 + z_2^2)^{0.5}}g_{hs}(\sigma)dz_2 \times \int_0^{\infty}\delta(C)\exp\left(\frac{\varphi_{hs}((r_2^2 + z_2^2)^{0.5})}{kT}\right)r_2dr_2\right] \tag{33}$$

where $C = ((r_2^2 + z_2^2)^{0.5} - \sigma)$ and $g_{hs}(\sigma)$ is the value of the hard-sphere radial distribution function at the contact point. The second integral in Eq. 33 is equal to unity when $C = 1$ and otherwise it is zero. Let us also change the upper limit of the first integral appearing in Eq. 33 to zero because we want just to consider the interaction of the molecules in a one side of the imaginary plate (note that the definition of the pressure is arbitrary). The result will be simplified to the following equation

$$P_{zz}^{FF} = \pi kT(\sigma)^{0.5}\rho_{hs}(z_1)\int_{-\sigma}^{0}\rho_{hs}(z_2)g_{hs}(\sigma)z_2^2dz_2$$

We do not presently have the expression for the contact hard-sphere radial distribution function $g_{hs}(\sigma)$ in nanoslits. We expect it to be different from the bulk system contact value while it is also a function of local density in the nanoslit. If we assume $\langle g_{hs}(\sigma)\rangle$ represents the average value of $g_{hs}(\sigma)$ in the nanoslit we can calculate $P_{zz}^{FF}/\langle g_{hs}(\sigma)\rangle$, i.e.,

$$P_{zz}^{FF}/\langle g_{hs}(\sigma)\rangle = \pi kT(\sigma)^{0.5}\rho_{hs}(z_1)\int_{-\sigma}^{0}\rho_{hs}(z_2)z_2^2dz_2$$

at various densities and nanoslit widths. Of course $\langle g_{hs}(\sigma)\rangle$ will be still a function of the bulk fluid density in equilibrium with the fluid in the nanoslit. Figure 3 shows the ratio $P_{zz}^{FF}/\langle g_{hs}(\sigma)\rangle$ as a function of z_1 position for various values of H/σ and $\rho\sigma^3$. Since the fluid in a nanopore is inhomogeneous, therefore, the molecules are not exposed to symmetric forces from the other molecules. According to Fig. 3 the ratio $P_{zz}^{FF}/\langle g_{hs}(\sigma)\rangle$ has the oscillatory behavior in the nanoslit pore. The values of the $P_{zz}^{FF}/\langle g_{hs}(\sigma)\rangle$ has a maximum and minimum (the extrema occurs at $(z_1/2)\sigma$ where z_1 is an integer). Remember that this figure shows the average force acting normal to the surface, where the forces are caused by atoms on one side of the surface interacting with atoms on the other side. If we insert the imaginary plane at $z = 0$, therefore no forces act though such surface from the left side.

In Fig. 3 we report the contribution of fluid-fluid interaction to the normal pressure at various pore width and at constant reduced dimensionless density $\rho\sigma^3 = 0.8$. We also report the contribution of the interactions between fluid–fluid molecules in the normal component of the pressure tensor at $H/\sigma = 6$ and $\rho\sigma^3 = 0.3, 0.6, 0.8$. We see that when the local density decreases the pressure profile becomes smooth and the height and depth of oscillations are reduced (see Fig. 3), furthermore.

2.8 The normal pressure tensor for hard-sphere fluids in nanoslit pores

Considering Eq. 27 for $\phi_{\text{ext}}^{hs}(r_{1z})$ we can conclude that the wall–fluid interaction term $P_{zz}^{\text{FW}} = \frac{\partial\phi_{\text{ext}}(r_{1z})}{\partial r_{1z}}\rho(r_{1z})$ for

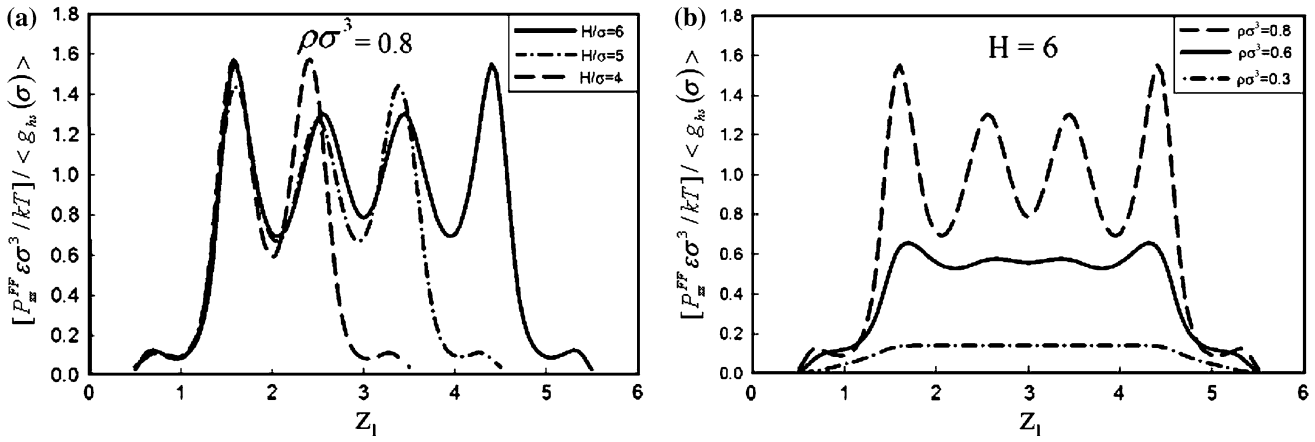

Fig. 3 Variation of $\left[P_{zz}^{FF}\varepsilon\sigma^3/kT\right]/\langle g_{hs}(\sigma)\rangle$ versus z_1, the distance from the wall: **a** At dimensionless bulk density $\rho\sigma^3 = 0.8$ but at various dimensionless nanoslit widths H/σ (H/σ = 6, 5, 4). **b** At H/σ = 6 but at various dimensionless bulk densities $\rho\sigma^3$ ($\rho\sigma^3$ = 0.8, 0.6, 0.3)

hard-sphere molecules in nanoslits is zero. This indicates that the normal pressure tensor of hard-sphere particles confined between the hard walls do not have any contribution from the walls. Therefore, the total normal pressure tensor in the confined hard-sphere system is equal to:

$$P_{zz}^{hs} = \rho(z_1)kT + \pi kT(\sigma)^{0.5}\rho_{hs}(z_1)\int_{-\sigma}^{0}\rho_{hs}(z_2)g_{hs}(\sigma)z_2^2\mathrm{d}z_2 \tag{34}$$

Due to our lack of knowledge about $g_{hs}(\sigma)$ and even $\langle g_{hs}(\sigma)\rangle$ we ae not presently able to calculate the exact value of the total normal pressure tensor for hard-spheres confined in nanoslit pores. However, considering the fact that both $P_{zz}^{K}\varepsilon\sigma^3/kT$ and $P_{zz}^{\mathrm{FW}}\varepsilon\sigma^3/kT$ indicate the existence of six distinct layers, we expect $P_{zz}\varepsilon\sigma^3/kT$ to possess also six distinct layers. To get an approximate idea about $P_{zz}\varepsilon\sigma^3/kT$, the z component of the pressure in the direction normal to the wall, we have plotted Fig. 4 assuming $\langle g_{hs}(\sigma)\rangle = 1$. We see that the pressure has different values between the walls and shows the oscillatory behavior. Also, we plot the normal pressure versus position z_1 for various pore width and reduced bulk density. Our result shows, the oscillatory form of the normal pressure tensor versus distance of the walls has been observed for very high densities. As the densities decreased, the height and depth of the oscillation is reduced.

3 Conclusions

It is well known that a confined fluid in a nanoslit pore is inhomogeneous and its thermodynamics properties are functions of the local density. We have derived an analytic equation for the local normal pressure tensor of a confined fluid in a nanoslit pore as a function of distance from the

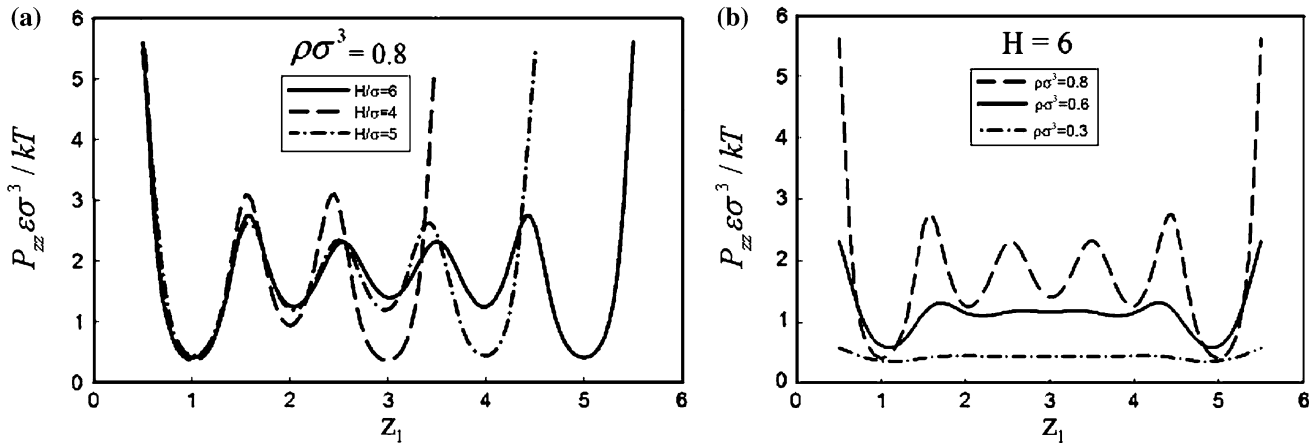

Fig. 4 Dimensionless normal pressure tensor $P_{zz}\varepsilon\sigma^3$/kT of hard sphere versus distance from the wall assuming $\langle g_{hs}(\sigma)\rangle = 1$. **a** At dimensionless bulk densities $\rho\sigma^3 = 0.8$ but at various dimensionless nanoslit widths H/σ (H/σ = 6, 4, 5). **b** At H/σ = 6 but at various dimensionless bulk densities $\rho\sigma^3$ ($\rho\sigma^3$ = 0.8, 0.6, 0.3)

wall. The confined fluid is assumed to be in equilibrium with a bulk (macroscopic) fluid system with known uniform density and temperature. The resulting normal pressure tensor equation is applicable for any fluid that is confined in a nano slit pore and with a any intermolecular pair-potential energy and fluid-wall interaction potential function.

The normal pressure tensor is composed of three parts, which include the kinetic contribution due to momentum of the particles, the contribution resulting from the force due to fluid-fluid two-body interactions and the contribution due to fluid–wall interaction.

We have calculated the normal component of the pressure tensor for the hard-sphere fluid confined between two parallel–structureless hard walls at different nanometer distances and at various uniform bulk densities. The choice of hard-sphere fluid is due to the availability of density profile data which we have generated recently and the fact that its configurational behavior is similar to other molecular confined fluids at.

Our computational results indicate that the kinetic contribution of the pressure tensor shows an oscillatory behavior and has a maximum at the contact point to the walls. When the local density decreases the layers become more diffuse and broad. Therefore, the pressure between the walls decreases but maintains its oscillatory behavior. When the pore width increases the layers of the molecules in the pore increase but the height of the layers decrease.

We also report the fluid-fluid interaction contribution to the normal component of pressure tensor at different local densities and pore widths. The results indicate that this contribution also has an oscillatory behavior inside the pore. When the local density decreases this profile becomes smooth and the height and depth of the oscillation are reduced.

There is no fluid–wall interaction contribution to the normal component of the pressure tensor of a hard-sphere confined fluid. This is because the hard-sphere particles confined between hard walls are not exposed to any force from the walls.

References

Brovchenko I, Geiger A, Oleinikova A (2004) Water in nanopores: II. Coexistence curves from Gibbs ensemble Monte Carlo simulation. J Chem Phys 120:1958

Carbajal-Tinoco MD, Castro-Roman F, Arauz-Lara JL (1996) Static properties of confined colloidal suspensions. Phys Rev E 53:3745–3749

Chen LJ, Ely JF, Mansoori GA (1987) Mean density approximation and hard-sphere expansion theory. Fluid Phase Equilib 37:1–27

Fisher IZ, Switz TM (1964) Statistical theory of liquids. University of Chicago Press, Chicago

Fortini A, Dijkstra M (2006) Phase behaviour of hard sphere confined between parallel hard plates: manipulation of colloidal crystal structure by confinement. J Phys Cond Matter 18:371–378

Fu D (2006) Investigation of excess adsorption, solvation force, and plate–fluid interfacial tension for Lennard–Jones fluid confined in slit pores. J Chem Phys 124:164701

Gotzelmann M, Dietrich S (1996) Density profiles and pair correlation function of hard sphere in narrow silts. Phys Rev E 55:2993–3005

Irving JH, Kirkwood J (1950) The statistical mechanical theory of transport processes. IV. The equation of state. J Chem Phys 18(6):817–829

Kamalvand M, Keshavarzi E, Mansoori GA (2008) Behavior of the confined hard-sphere fluid within nanoslits: a fundamental-measure density-functional theory study. Int J Nanosci 7(4&5): 245–253

Kekicheff P, Richetti P (1992) Direct measurement of depletion and structural forces in a micellar system. Phys Rev Lett 68:1951–1954

Keshavarzi T, Sohrabi R, Mansoori GA (2006) An analytic model for nano confined fluids phase-transition: applications for confined fluids in nanotube and nanoslit. J Comput Theor Nanosci 3(1):134–141

Mansoori GA (1977) Thermodynamics of systems at high pressures (Soft-Sphere Model). In: Seventh thermophysical properties symposium series, pp 442–450

Mansoori GA (2005) Principles of nanotechnology: molecular-based study of condensed matter in small systems. World Science Publication Co., Hackensack

Mansoori GA, Canfield FB (1970) Perturbation and variational approaches to the equilibrium thermodynamic properties of liquids and phase transitions. Ind Eng Chem (Monthly) 62(8): 12–29

Mansoori GA, Kioussis N (1985) A new thermodynamic model for the hard-core fluid with a Yukawa Tail. J Chem Phys 82:2076–2081

Parker JL, Richetti P, Kekicheff P, Sarman S (1992) Direct measurement of structural forces in a supermolecular fluid. Phys Rev Lett 68:1955–1958

Schmidt M, Lowen H (1997) Phase diagram of hard spheres confined between two parallel plates. Phys Rev E 55(6):7228–7241

Zhang W, Li D (2007) Simulation of low speed 3D nanochannel flow. Microfluidics Nanofluidics 3(4):417–425

Ziarani AS, Mohamad AA (2006) A molecular dynamics study of perturbed Poiseuille flow in a nanochannel. Microfluidics Nanofluidics 2(1):12–20